RSC Advances

PAPER

View Article Online
View Journal | View Issue

Cite this: *RSC Adv.*, 2022, **12**, 31976

Lithium sensors based on photophysical changes of 1-aza-12-crown-4 naphthalene derivatives synthesized *via* Buchwald–Hartwig amination†

Haneul Kim and Byungjin Koo *

Lithium detection is of great significance in many applications. Lithium-sensing compounds with high selectivity are scarce and, if any, complicated to synthesize. We herein report a novel yet simple compound that can detect lithium ions in an organic solvent through changes in absorbance and fluorescence. Naphthalene functionalized with 1-aza-12-crown-4 (**1**) was synthesized *via* one step from commercially available 1-bromonaphthalene through Buchwald–Hartwig amination. In order to obtain a structure–property relationship, we also synthesized two other compounds that are structurally similar to **1**, wherein the compounds **2** and **3** include an imide moiety (an electron acceptor) and do not include a 1-aza-12-crown-4 unit, respectively. Upon the addition of lithium ions, compound **1** displayed a clear isosbestic point in the absorption spectra and a new peak in the fluorescence spectra, whereas the compounds **2** and **3** indicated miniscule and no spectroscopic changes, respectively. ^{1}H NMR titration studies and the calculated optimized geometry from density functional theory (DFT) indicated the lithium binding on the aza-crown. The calculated limit of detection (LOD) was 21 μM. The lithium detection with **1** is selective among other alkali metals (Na^{+}, K^{+}, and Cs^{+}). DFT calculation indicated that the lone pair electrons in the nitrogen atom of **1** is delocalized yet available to bind lithium, whereas the nitrogen lone pair electrons of **2** showed significant intramolecular charge transfer to the imide acceptor, resulting in a high dipole moment, and thus were unavailable to bind lithium. This work elucidates the key design parameters for future lithium sensors.

Received 12th September 2022
Accepted 2nd November 2022

DOI: 10.1039/d2ra05746h

rsc.li/rsc-advances

1. Introduction

For advanced electronic technology,[1,2] lithium has served as one of the most important elements in the past few decades. Due to the surging demand fpr lithium-ion batteries used in personal electronics and electric vehicles, lithium extraction technology is garnering tremendous attention for sustainable production of lithium. Lithium is extracted from primary sources (*e.g.*, lithium-rich brine) as well as from secondary sources (*e.g.*, spent lithium-ion batteries), wherein organic solvents such as PC-88A serve as extractants that acquire lithium from aqueous solution.[3–5] To determine the lithium concentration in the extracted organic phase, generally ranging from a few to hundreds of millimolar concentrations, instruments such as ICP-OES (inductively coupled plasma-optical emission spectroscopy) are currently employed.[6–8] However, these instruments require prolonged sample preparation steps and measurement time. Therefore, methods that enable more efficient and prompt determination of lithium concentrations need to be developed.

Various lithium sensing strategies, such as electrochemical detection,[9–12] fiber-based sensors,[13] a flow-through optode,[14] and photophysical (absorbance and fluorescence) transduction,[15–19] have been developed. Among them is the photophysical method that exhibits superior utility owing to the apparent optical changes without interpretation of complex data, fast measurement time, and facile sample preparation procedures. The working principles of these spectroscopic lithium sensors are grounded on chelation-induced photophysical changes,[20,21] including intramolecular charge transfer (ICT),[22] photoinduced electron transfer (PET),[23] Forster resonance energy transfer (FRET),[24] and excited-state intramolecular proton-transfer (ESIPT).[25] To build the optical sensors, chemists design a sensor that consists of two parts: an ionophore for selective lithium binding and a chromophore/fluorophore for optical changes.[21,26] While various lithium-chelating ligands have been developed including porphyrins,[27,28] phenanthrolines,[29] and calixarenes,[30,31] crown ethers and their derivatives[32–35] are known to show strong affinity to lithium over sodium and potassium, particularly in the case of 12-crown-4 and 14-crown-4 given the cavity size. Chromo- and fluorophores are small molecular dyes, such as acenes,[36] squaraine

Department of Polymer Science and Engineering, Dankook University, Yongin, Gyeonggi 16890, Republic of Korea. E-mail: bkoo@dankook.ac.kr

† Electronic supplementary information (ESI) available. See DOI: https://doi.org/10.1039/d2ra05746h

dyes,[37] BODIPY,[38,39] coumarins,[16,40] quinoxaline,[41] and naphthalimides.[17] However, these probes functionalized with crown ethers often possess complex molecular structures that require multiple synthetic steps to prepare.

Herein, we report a structurally simple lithium sensor (**1**, referred to as Naph-Crown) containing naphthalene with 1-aza-12-crown-4 (Fig. 1a). In spite of the simplicity, this molecule has never been reported. To understand the structure–property relationship, we also designed and synthesized the compounds **2** (NMI-Crown, wherein NMI stands for naphthalene monoimide) and **3** (NMI-Br) (Fig. 1a). Our initial hypothesis was that the compound **2** was believed to undergo ICT upon photoexcitation with the appearance of a longer absorption band (ICT band), which would disappear if lithium were bound to the crown ether. However, we observed minute absorbance and fluorescence changes. Unexpectedly, the compound **1** exhibited unequivocal ratiometric absorbance changes and the generation of a new fluorescence peak (Fig. 1b). The sensor was not responsive to Na^+, K^+, and Cs^+ in both absorbance and fluorescence, presenting selectivity among alkali metals. An additional advantage of the sensor **1** is that it can be readily synthesized only one step from a commercially available starting material through Buchwald–Hartwig amination, suggesting the great possibility of practical applications and commercialization.

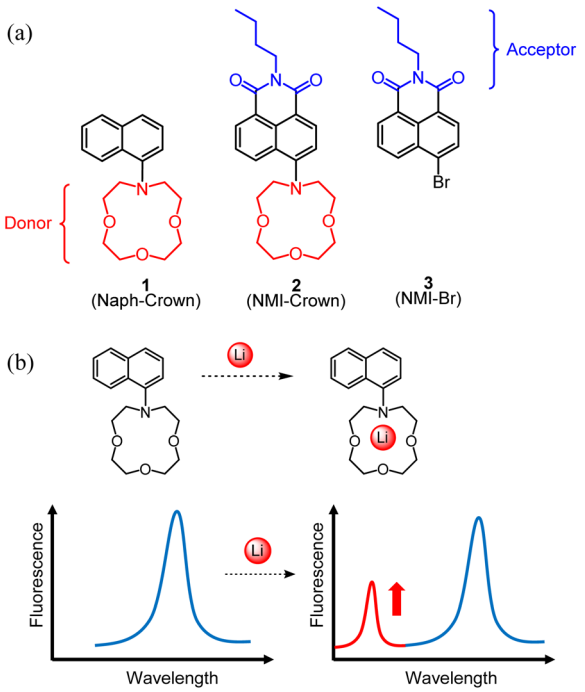

Fig. 1 Overview of this work. (a) Three naphthalene derivatives with a donor (**1**), a donor–acceptor (**2**), and an acceptor (**3**), were synthesized to test a response to lithium ions. (b) The Naph-Crown **1** showed ratiometric absorption/fluorescence responses (only fluorescence was indicated) upon the addition of lithium, whereas the NMI-Crown (**2**) with a strong ICT characteristic had miniscule responses. NMI-Br (**3**) was used as a control sensor lacking a crown ligand.

2. Materials and methods

2.1 General

Chemicals were purchased from Sigma-Aldrich, TCI, Daejung Chemicals, Samchun Chemicals, and Duksan Chemicals without further purification unless noted otherwise. All reactions were carried out under argon with standard Schlenk techniques. Dry solvents were prepared with activated 4 Å molecular sieves. All ^{1}H NMR and ^{13}C NMR are reported in ppm on a JEOL ECS 400 MHz NMR spectrometer. ^{1}H NMR is referenced to a chloroform peak (δ = 7.26 ppm) or an acetonitrile peak (δ = 1.94 ppm) for NMR titration studies with lithium. The multiplicity is reported as follows: s = singlet, d = doublet, dd = doublet of doublet, t = triplet, m = multiplet or unresolved, br = broad. Coupling constants J are reported in Hz. ^{13}C NMR is referenced to chloroform (δ = 77.16 ppm). High-resolution mass spectrometry (HRMS) using electrospray ionization (ESI) in a positive mode was performed with AB SCIEX Q-TOF 5600. UV-vis spectra were recorded on a Scinco Mega U600 UV-vis spectrophotometer at room temperature. Fluorescence measurements were performed at room temperature with a Hitachi F-7000 (150 W xenon lamp).

2.2 Synthesis of 1 (Naph-Crown)

To the flame-dried Schlenk flask, 1-bromonaphthalene (0.97 mmol, 1.00 equiv., 200 mg), 1-aza-12-crown-4 (1.11 mmol, 1.14 equiv., 193 mg), $Pd_2(dba)_3$ (0.0097 mmol, 0.01 equiv., 9 mg), DavePhos (0.058 mmol, 0.06 equiv., 23 mg), and NaO*t*Bu (1.35 mmol, 1.4 equiv., 130 mg) were dissolved in 1.7 mL of dry toluene, and this mixture was degassed with argon. The reaction mixture was heated and stirred at 90 °C for 25 h. After cooling down to room temperature, the solvent was evaporated *in vacuo*. The mixture was purified with column chromatography (hexane : ethyl acetate = 1 : 1), producing a dark yellow oil (185 mg, 63% yield). ^{1}H NMR (400 MHz, $CDCl_3$) δ 8.66 (d, J = 8.2 Hz, 1H), 7.82 (dd, J = 7.4, 1.8 Hz, 1H), 7.56 (d, J = 8.1 Hz, 1H), 7.54–7.43 (m, 2H), 7.40 (t, J = 7.8 Hz, 1H), 7.23 (d, J = 7.4 Hz, 1H), 3.83–3.73 (m, 12H), 3.46 (t, J = 4.8 Hz, 4H). ^{13}C NMR (101 MHz, $CDCl_3$) δ 149.21, 135.11, 130.79, 128.11, 125.89, 125.63, 125.40, 124.77, 123.71, 117.89, 71.55, 71.05, 70.18, 54.66. HRMS (ESI) calculated for $C_{18}H_{24}NO_3$ ($[M + H]^+$) 302.1751; found, 302.1747.

2.3 Synthesis of 2 (NMI-Crown)

To the flame-dried Schlenk flask, *N*-butyl-4-bromo-1,8-naphthalimide (0.60 mmol, 1.00 equiv., 200 mg), 1-aza-12-crown-4 (0.68 mmol, 1.14 equiv., 120 mg), $Pd_2(dba)_3$ (0.006 mmol, 0.01 equiv., 5.5 mg), DavePhos (0.036 mmol, 0.06 equiv., 14 mg), and NaO*t*Bu (0.840 mmol, 1.4 equiv., 81 mg) were dissolved in 1.5 mL of dry toluene, and this mixture was degassed with argon. The reaction mixture was heated and stirred at 100 °C for 20 h. After cooling down to room temperature, the solvent was evaporated *in vacuo*. The mixture was purified with column chromatography (dichloromethane : ethyl acetate = 1 : 1), producing a dark yellow solid (75 mg, 29% yield). Melting point 60–61 °C. ^{1}H NMR (400 MHz, $CDCl_3$) δ 9.09

(d, J = 8.5 Hz, 1H), 8.58 (d, J = 7.2 Hz, 1H), 8.49 (d, J = 8.2 Hz, 1H), 7.68 (t, J = 8.1 Hz, 1H), 7.31 (br, 1H), 4.17 (t, J = 7.8 Hz, 2H). 3.90–3.55 (m, 16H), 1.76–1.62 (m, 2H), 1.50–1.37 (m, 2H), 0.96 (t, J = 7.3 Hz). ^{13}C NMR (101 MHz, $CDCl_3$) δ 164.68, 164.10, 132.07, 131.99, 131.25, 130.48, 127.10, 125.41, 122.93, 115.61, 71.31, 71.26, 69.12, 54.35, 40.08, 30.32, 20.47, 13.95. HRMS (ESI) calculated for $C_{24}H_{31}N_2O_5$ ($[M + H]^+$) 427.2227; found, 427.2226.

2.4 Synthesis of 3 (NMI-Br)

To the flame-dried Schlenk flask, 4-bromo-1,8-naphthalic anhydride (3.6 mmol, 1.00 equiv., 1 g) was added and dissolved in 8.3 mL of ethylene glycol. *n*-Butylamine (5.4 mmol, 1.5 equiv., 0.53 mL) was added, and the mixture was stirred at 160 °C for 12 h. After cooling down to room temperature, 2 M HCl (aq.) was added, and the mixture was extracted three times with dichloromethane. The combined organic phase was dried over $MgSO_4$, filtered, and concentrated *in vacuo*. The crude mixture was purified with column chromatography (hexane : ethyl acetate = 4 : 1), producing an off-yellow solid (1.07 g, 89% yield). Melting point 99 °C. ^{1}H NMR (400 MHz, $CDCl_3$) δ 8.67 (dd, J = 7.3, 1.2 Hz, 1H), 8.58 (dd, J = 8.7, 1.3 Hz, 1H), 8.42 (d, J = 7.8 Hz, 1H), 8.05 (d, J = 7.8 Hz, 1H), 7.86 (dd, J = 8.6, 7.4 Hz, 1H), 4.18 (t, J = 7.8 Hz, 2H), 1.76–1.66 (m, 2H), 1.51–1.39 (m, 2H), 0.98 (t, J = 7.3 Hz, 3H).

2.5 DFT calculation

The ORCA 5.0 software program[42] was used to calculate frontier molecular orbitals. The gas-phase ground state molecular geometry optimizations were carried out in B3LYP hybrid exchange–correlation functional[43] with the 6-31G* basis set.[44] Cartesian coordinates of optimized structures of the compounds **1**, **2**, and **1** + LiCl were included in ESI.† Avogadro software program was used to display HOMO and LUMO.

2.6 Photophysical analysis

Naph-Crown, NMI-Crown, and NMI-Br were dissolved in acetonitrile (ACN) at a concentration of 0.01 or 0.025 mM (for absorption) and 0.1 mM (for fluorescence). Lithium perchlorate with a concentration of 100 mM was prepared in ACN. For the UV-vis and fluorescence experiments, 2 mL of the solution was aliquoted into a quartz cuvette, and the lithium solution was subsequently added. The experiments with other alkali metals were performed in an identical way with perchlorate salts. For potassium and cesium, the saturated solutions were used.

3. Results and discussion

We employed naphthalene as a chromo/fluorophore and 1-aza-12-crown-4 as a selective ligand for lithium. Although various naphthalene-based dyes have been developed,[45] Naph-Crown (**1**) in this work has never been reported. This molecule possesses a nitrogen atom that is moderately conjugated to the naphthalene ring (Fig. 1a). To understand the effect of lithium

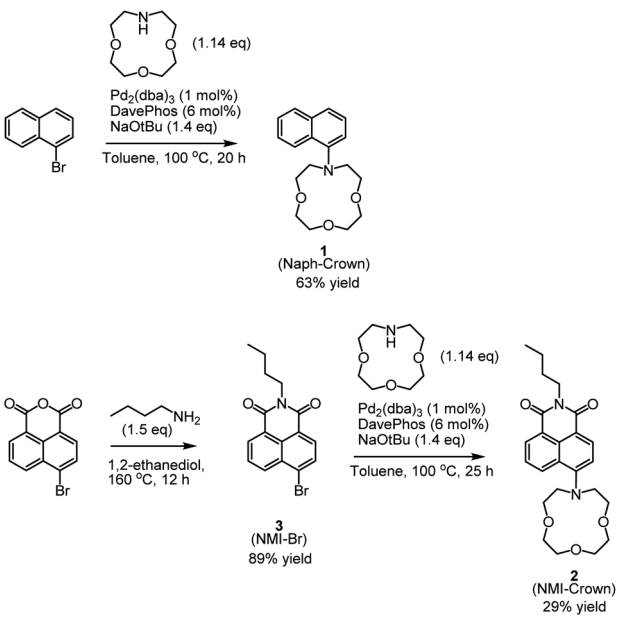

Scheme 1 Synthetic procedures to prepare the compounds **1**, **2**, and **3** through Buchwald–Hartwig amination.

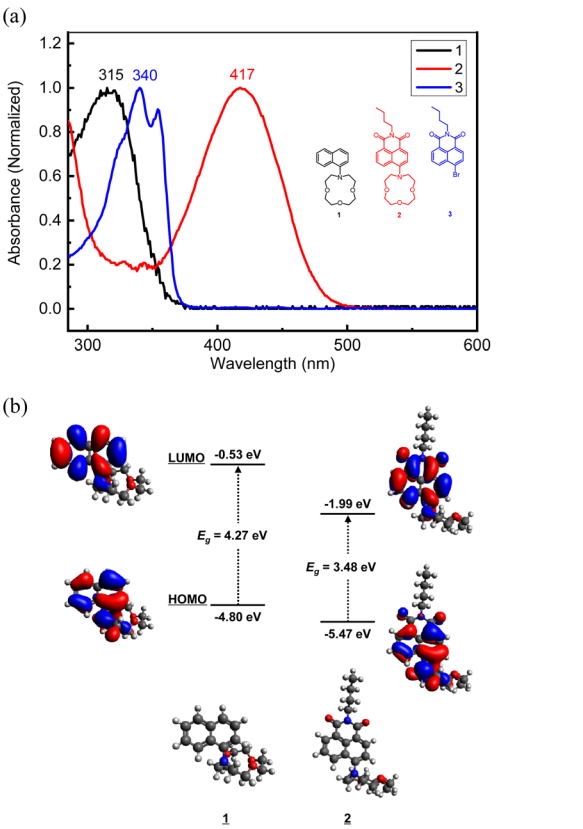

Fig. 2 (a) UV-vis spectra of the compounds **1**, **2**, and **3**. Naph-Crown (**1**) showed an absorption maximum at 315 nm, and NMI-Crown (**2**) indicated the significantly red-shifted maximum at 417 nm due to strong ICT. NMR-Br (**3**) had an absorption maximum at 340 nm. (b) DFT calculation and frontier molecular orbitals. Owing to the electron acceptor, HOMO and LUMO levels were lowered and LUMO of **2** was shifted to the imide moiety.

chelation and ratiometric sensor responses, we additionally prepared an ICT-type molecule, NMI-Crown (**2**). Generally, ICT-type sensors are known to exhibit clear ratiomentric sensor responses,[46–49] although our result indicated disparate behaviors (*vide infra*). The NMI-Br (**3**) lacking the crown ether was selected as a control molecular sensor.

The syntheses of the compounds **1**, **2**, and **3** were shown in Scheme 1. For the synthesis of **1**, Buchwald–Hartwig cross-coupling reactions were considered,[50,51] and previously, *N*-aryl-aza-crown ethers were prepared using a DavePhos ligand with high yields.[52] Hence, we used a similar Buchwald–Hartwig condition. The reaction was begun with a commercially available 1-bromonaphthalene that reacted with 1-aza-12-crown-4 in the presence of $Pd_2(dba)_3$ (1 mol%), DavePhos (6 mol%), and NaO*t*Bu (1.4 equiv.) in toluene. The isolated yield was 63%. For the synthesis of **2**, 4-bromo-1,8-naphthalic anhydride was treated with *n*-butylamine to form **3** containing a naphthalene monoimide (NMI) skeleton, followed by the Buchwald–Hartwig amination with the same condition as in **1**, resulting in the production of **2** with the isolated yield of 29%. The compounds **1** and **2** were characterized by ^{1}H NMR, ^{13}C NMR, and HRMS.

The UV-vis spectra of each compound were measured in acetonitrile (Fig. 2a). Naph-Crown (**1**) showed the absorption maximum at 315 nm, which was red-shifted about 40 nm from naphthalene.[53] This red-shift may be attributed to the extended conjugation from the nitrogen atom in the naphthalene ring. NMI-Crown (**2**), having an acceptor imide moiety, exhibited the absorption maximum at 417 nm, which was far red-shifted from **1** by more than 100 nm. This large red-shift is related to a strong ICT characteristic of the donor–acceptor type molecule **2**. Density functional theory (DFT) calculation in B3LYP functional with 6-31G* basis set indicated the lowered HOMO (from −4.80 to −5.47 eV) and LUMO (from −0.53 eV to −1.99 eV) due to the electron-withdrawing group (Fig. 2b). In addition, the shape of LUMO of **2** was shifted to the imide moiety and the dipole moments of **1** and **2** were calculated to be 2.78 D and 7.18 D, respectively, suggesting the formation of strong ICT upon photoexcitation. NMI-Br (**3**), wherein the crown ether was replaced with a bromine atom, exhibited the absorption maximum at 340 nm, which was far blue-shifted from **2** owing to the diminished ICT character.

To investigate the lithium binding effect, we measured UV-vis spectra upon the addition of lithium salt solutions (lithium perchlorate) in each compound (Fig. 3). We used acetonitrile as a model organic solvent. The concentration of the compounds was kept at 0.01 mM, and the lithium salt concentration of 100 mM in acetonitrile was prepared. Upon the addition of the lithium solution to Naph-Crown (**1**), we observed

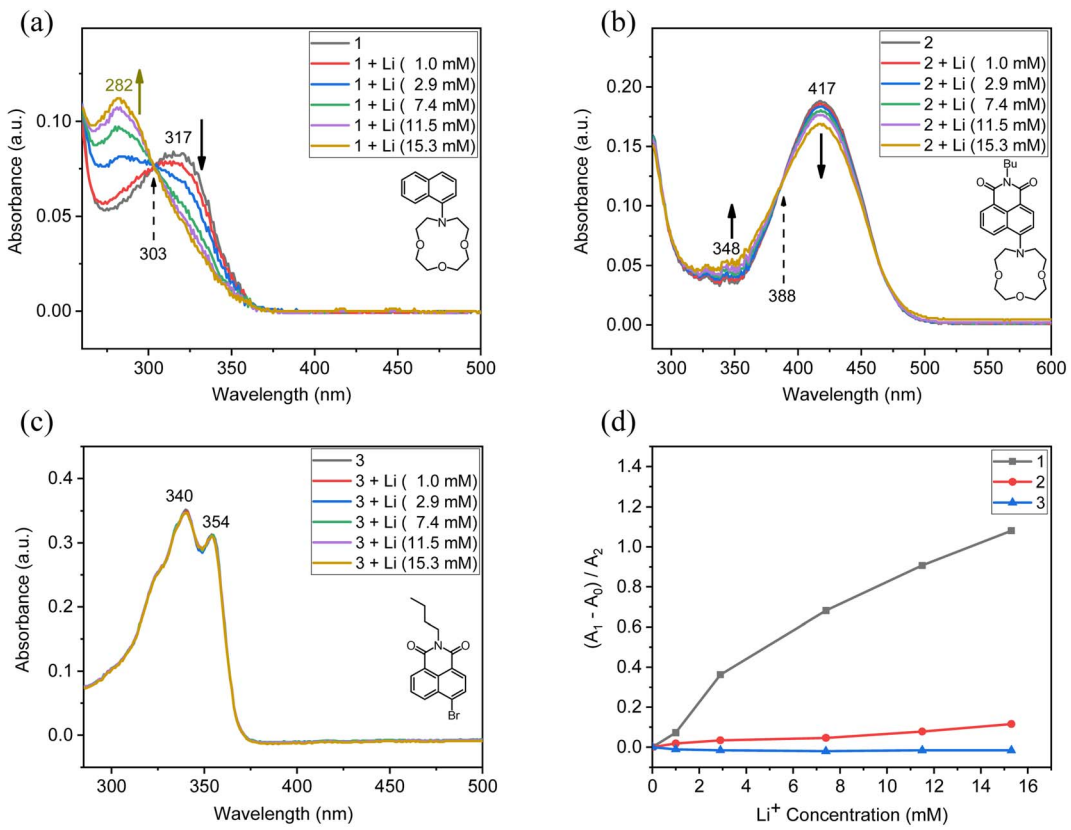

Fig. 3 UV-vis spectra with added lithium ions. The concentration of the compound **1**, **2**, and **3** was kept constant at 0.01 mM. (a) UV-vis spectra of **1** with lithium ions. The appearance of the new blue-shifted peak at 282 nm could be attributed to the local naphthalene absorption in which the nitrogen atom was not conjugated. (b) UV-vis spectra of **2** with lithium ions. Due to strong ICT, binding of lithium and spectral changes were minimal. (c) UV-vis spectra of **3** with lithium ions, wherein the absence of a crown ether resulted in no spectral changes. (d) Summarized sensor responses based on the relative absorption changes over the lithium concentrations.

the decrease of the peak at 317 nm, while a new peak at 282 nm was generated (Fig. 3a). A clear isosbestic point was observed at 303 nm, indicating that two species are responsible for this change. The blue-shifted new peak at 282 nm could be attributed to the naphthalene absorption without the conjugation of the lone pair electrons on the nitrogen atom owing to the chelation to lithium. The binding constant (K) of the compound **1** with lithium was calculated based on the following equation, $\Delta A = [D]\Delta\varepsilon[M]/((1/K) + [M])$,[54] wherein ΔA, [D], [M], $\Delta\varepsilon$, and K represent the absorption difference at a particular wavelength upon the addition of metal ions, the dye concentration (herein Naph-Crown), the metal ion concentration, the change in extinction coefficient upon the addition of metal ions, and the binding constant, respectively. The resulting plot produced the binding constant of 127 M^{-1} for the association between the compound **1** and lithium (Fig. S1†). In the case of NMI-Crown (**2**), there was a miniscule ratiometric change in which the absorption at 417 nm was slightly decreased with the increased signal at 348 nm (Fig. 3b). An isosbestic point at 388 nm was observed. On the contrary to the previous reports on ICT-type sensors with excellent properties,[46–49] we found that in our case the strong ICT feature leading to reduced basicity of nitrogen may be detrimental to sensing properties. For NMI-Br (**3**) without the crown ether, the absorption spectra presented no changes upon the lithium addition, demonstrating that the crown ether is necessary for sensor responses (Fig. 3c). We calculated the relative absorbance change rate, $(A_1 - A_0)/A_2$, and plotted this rate (y-axis) over the lithium concentration (x-axis), wherein A_0, A_1, and A_2 represent the decreasing absorption (at 317, 417, and 354 nm in each of **1**, **2**, and **3**), the increasing absorption (at 282, 348, and 340 nm, *ditto*), and the initial absorption without lithium (at 317, 417, and 354 nm, *ditto*), respectively (Fig. 3d). The graph explicitly represents the high sensitivity of **1** (black curve) in comparison to **2** (red) and **3** (blue).

To confirm the binding of lithium to a crown-ether moiety on **1**, we performed the ^{1}H NMR titration studies (referenced to CD_3CN at 1.94 ppm) and DFT calculation (Fig. 4). The ^{1}H chemical shifts of the crown-ether moiety near 3.3–3.8 ppm exhibited significant peak broadening with the downward chemical shift (Fig. 4a), implying that there may be fast associative/dissociative equilibrium between the lithium and the crown-ether, which could not be differentiated in the NMR time scale. The peak broadening was relatively insignificant in the naphthyl unit (Fig. 4b). The DFT calculation of the compound **1** and lithium (chloride as anion for charge neutrality) in B3LYP/6-31G* produced the optimized geometry (Fig. 4c), wherein the lithium (purple) is coordinated to four heteroatoms of the crown-ether with the distances of 2.00–2.45 Å. In addition, in order to examine the effect of cyclic etherial ligands, we synthesized the *n*-butylamine-substituted NMI (NMI–NH–Bu). This compound was not responsive to lithium ions (Fig. S2a†), further demonstrating that aza-crown-ether is necessary for lithium chelation.

A theoretical limit of detection (LOD) was estimated using the following equation: LOD = $3(RMS_{noise}/slope)$,[55] wherein RMS_{noise} represents a root-mean-square noise that was

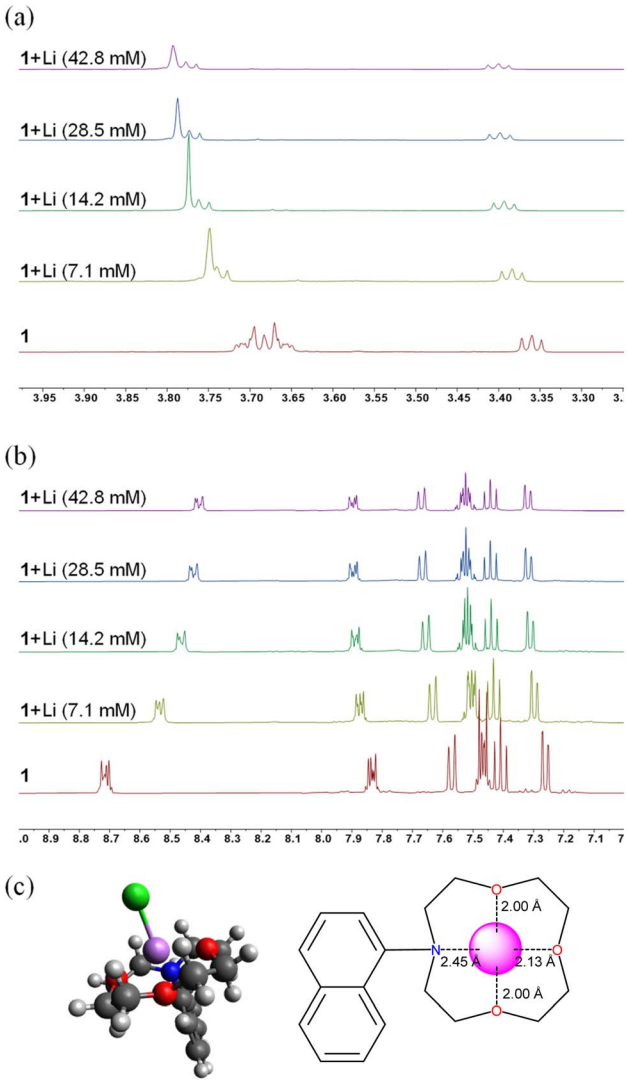

Fig. 4 NMR and DFT studies to elucidate the binding mode. The ^{1}H NMR chemical shifts of **1** with the different concentrations of lithium ions in the region of (a) the crown-ether moiety and (b) the naphthyl unit were displayed. The chemical shifts of the crown-ether moiety showed significant peak broadening. (c) DFT calculation (B3LYP/6-31G*) indicated the lithium (purple) binding to the crown-ether moiety. The distances were shown in the optimized geometry. Chloride (green) was added for charge neutrality.

calculated by taking ten blank measurements of the compound **1** (detailed procedure was described in ESI†). The slope was obtained in the concentration–signal plot (black curve in Fig. 3d). The calculated LOD was 21 μM. Although this LOD is higher than the previously reported LOD values (*e.g.*, LOD of 5 μM from a naphthalene diimide derivative with two crown ethers),[17] our sensor can cover a wide range of applications that require lithium detection, along with the structural simplicity.

Next, fluorescence measurements were executed with lithium ions (Fig. 5). Naph-Crown (**1**) with lithium indicated a new peak at 337 nm (Fig. 5a), which was increasing with higher lithium concentrations (Fig. 5b). We suppose that this emission could be generated from a locally excited (LE) state

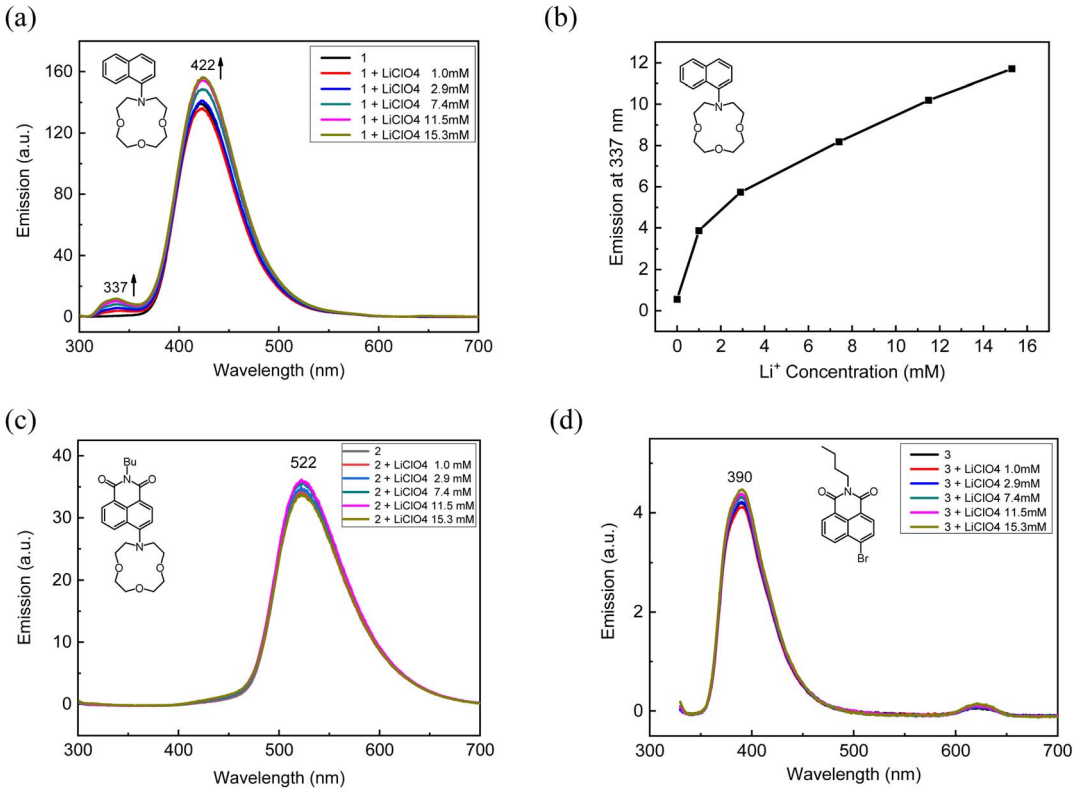

Fig. 5 Fluorescence spectra with the addition of lithium. (a) Naph-Crown (**1**) had a new blue-shifted peak at 337 nm in the presence of lithium ions, which is presumably generated from an LE state. Excitation at 280 nm was applied. (b) This emission intensity (height) at 337 nm was plotted over the lithium concentration. (c) NMI-Crown (**2**) indicated red-shifted emission due to ICT, and no new peak was observed with lithium ions. Excitation at 280 nm was applied. (d) NMI-Br (**3**) showed unchanged spectra with lithium, suggesting that the crown ether is a key moiety for lithium binding. Excitation at 310 nm was applied.

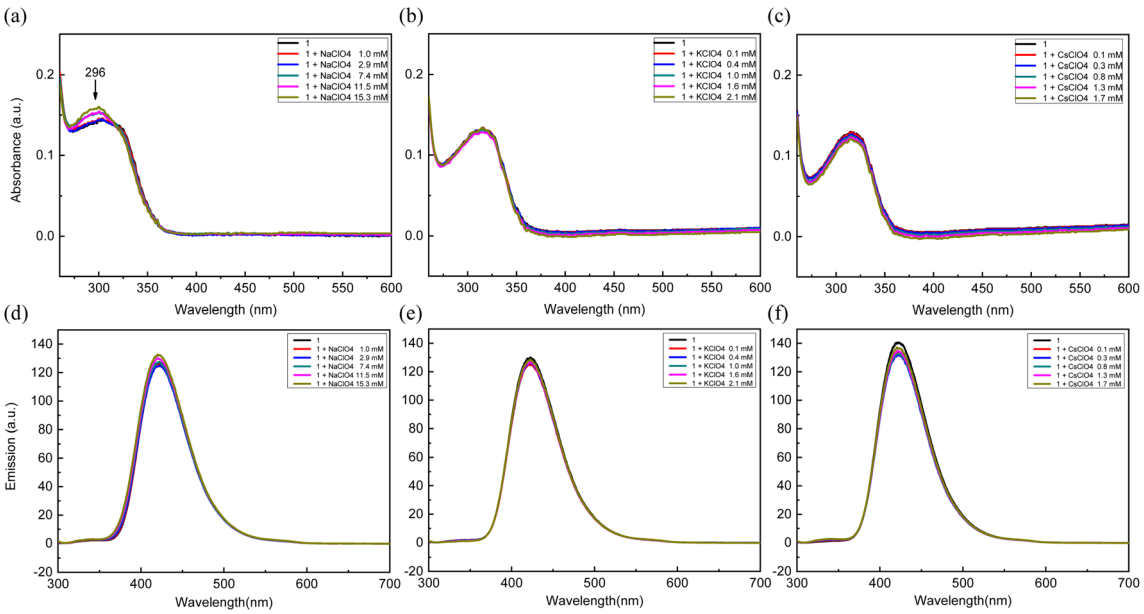

Fig. 6 UV-vis (top) and fluorescence spectra (bottom) of **1** with (a and d) Na^+, (b and e) K^+, and (c and f) Cs^+. No significant changes were observed, indicating that the sensor **1** is selective to Li^+ over Na^+, K^+, and Cs^+.

that is present when the lone pair electrons of the nitrogen atom in **1** is bound to lithium. Although it appeared that lithium was bound to **1** significantly given the UV-vis spectra, we still observed the large emission of **1** at 422 nm. It is worth mentioning that no self-quenching occurred at this concentration of 0.1 mM (Fig. S3†). The compound **2** has a longer-wavelength emission at 521 nm owing to the strong CT state. In contrast to **1**, no new peak was observed with the lithium addition (Fig. 5c). In the compound **3**, no significant emission changes were observed, repeatedly demonstrating that crown ether is necessary for lithium binding (Fig. 5d).

Having confirmed the absorption and emission changes with lithium in **1**, we performed selectivity tests with Na^+, K^+, and Cs^+ having the identical perchlorate counterions. In most cases, we found that the compound **1** was not responsive to the three alkali metal ions based on both absorption and emission spectra (Fig. 6), suggesting the excellent selectivity of the sensor **1** among alkali metals. It is worth noting that the sodium cation generated a weak new absorption signal at 296 nm (Fig. 6a). This is perhaps due to the weak interaction between the aza-crown-ether and sodium cation, as reported previously.[56,57] To test the binding of lithium in the presence of other alkali metals, lithium and sodium with a 1 : 1 molar ratio were mixed and added to the receptor **1**. A clear isosbestic point at 303 nm was still observed (Fig. S4†), presenting that the binding of lithium was effective in the presence of non-interacting alkali metals. A similar behavior was observed with potassium ions as well (Fig. S4†).

4. Conclusions

In this study, we report the synthesis of the molecular sensor **1** that can selectively detect lithium ions through photophysical changes. The compound **1**, possessing a naphthalene skeleton with 1-aza-12-crown-4, was synthesized through the Buchwald–Hartwig amination, requiring only one synthetic step from a commercially available starting material. Upon the addition of lithium, the sensor **1** indicated a ratiometric absorption change as well as generation of a new emission peak owing to the lithium binding. LOD was estimated to be 21 μM. Other alkali metals, including Na^+, K^+, and Cs^+, were rarely responsive. NMR studies and DFT calculations revealed the binding of lithium to the aza-crown ether on **1**. The compound **2**, having an imide acceptor and giving rise to the ICT, showed unnoticeable photophysical changes, suggesting that the strong ICT may not be beneficial to the fabrication of lithium sensor, in contrast to the conventional knowledge. Based on this structure–property relationship, we are currently synthesizing other lithium-sensing chromophores working in visible light which can be recognized by naked eyes for practical applications.

Conflicts of interest

The authors declare no competing financial interest.

Acknowledgements

This work was supported by the National Research Foundation of Korea (NRF) grant funded by the Korea government (MSIT) (2020R1G1A1102161). The Department of Polymer Science and Engineering was supported through the Research-Focused Department Promotion & Interdisciplinary Convergence Research Project as a part of the University Innovation Support Program for Dankook University in 2022. This work was also supported by Korea Institute for Advancement of Technology (KIAT) grant funded by the Korea Government (MOTIE) (P0002007, HRD Program for Industrial Innovation).

References

1 J. B. Goodenough and K.-S. Park, The Li-Ion Rechargeable Battery: A Perspective, *J. Am. Chem. Soc.*, 2013, **135**(4), 1167–1176.
2 J. R. Geddes, S. Burgess, K. Hawton, K. Jamison and G. M. Goodwin, Long-Term Lithium Therapy for Bipolar Disorder: Systematic Review and Meta-Analysis of Randomized Controlled Trials, *Am. J. Psychiatry*, 2004, **161**(2), 217–222.
3 P. Meshram, B. D. Pandey and T. R. Mankhand, Extraction of lithium from primary and secondary sources by pre-treatment, leaching and separation: a comprehensive review, *Hydrometallurgy*, 2014, **150**, 192–208.
4 B. Swain, Recovery and recycling of lithium: a review, *Sep. Purif. Technol.*, 2017, **172**, 388–403.
5 G. Liu, Z. Zhao and A. Ghahreman, Novel approaches for lithium extraction from salt-lake brines: a review, *Hydrometallurgy*, 2019, **187**, 81–100.
6 L. Zhang, L. Li, D. Shi, X. Peng, F. Song, F. Nie and W. Han, Recovery of lithium from alkaline brine by solvent extraction with β-diketone, *Hydrometallurgy*, 2018, **175**, 35–42.
7 A. Pálsdóttir, C. A. Alabi and J. W. Tester, Characterization of 14-Crown-4 Ethers for the Extraction of Lithium from Natural Brines: Synthesis, Solubility Measurements in Supercritical Carbon Dioxide, and Thermodynamic Modeling, *Ind. Eng. Chem. Res.*, 2021, **60**(21), 7926–7934.
8 B. Koo, L. E. Sofen, D. J. Gisch, B. Kern, M. A. Rickard and M. B. Francis, Lithium-Chelating Resins Functionalized with Oligoethylene Glycols toward Lithium-Ion Battery Recycling, *Adv. Sustainable Syst.*, 2021, **5**(2), 2000230.
9 A. L. Suherman, B. Rasche, B. Godlewska, P. Nicholas, S. Herlihy, N. Caiger, P. J. Cowen and R. G. Compton, Electrochemical Detection and Quantification of Lithium Ions in Authentic Human Saliva Using $LiMn_2O_4$-Modified Electrodes, *ACS Sens.*, 2019, **4**(9), 2497–2506.
10 A. Bakhtiarvand Bakhtiari, B. Mohammadi, P. Moazzam, D. Didehroshan and A. Razmjou, An Evolving Insight into the Progress of Material Design for Membrane-Based Electrochemical Lithium Ion Detection, *Adv. Mater. Interfaces*, 2021, **8**(19), 2100571.
11 M. Nel-lo, Ò. Ferrer, S. Colominas and J. Abellà, Lithium sensors based on $Li_6La_3Ta_{1.5}Y_{0.5}O_{12}$ and $Li_6BaLa_2Ta_2O_{12}$

garnet electrolytes for molten lead alloys, *Sens. Actuators, B*, 2021, **339**, 129831.
12 E. Zdrachek and E. Bakker, Potentiometric Sensing, *Anal. Chem.*, 2021, **93**(1), 72–102.
13 M. N. Sweilam, J. R. Varcoe and C. Crean, Fabrication and Optimization of Fiber-Based Lithium Sensor: A Step toward Wearable Sensors for Lithium Drug Monitoring in Interstitial Fluid, *ACS Sens.*, 2018, **3**(9), 1802–1810.
14 M. I. Albero, J. A. Ortuño, M. S. García, M. Cuartero and M. C. Alcaraz, Novel flow-through bulk optode for spectrophotometric determination of lithium in pharmaceuticals and saliva, *Sens. Actuators, B*, 2010, **145**(1), 133–138.
15 K. Hiratani, M. Kaneyama, Y. Nagawa, E. Koyama and M. Kanesato, Synthesis of [1]Rotaxane *via* Covalent Bond Formation and Its Unique Fluorescent Response by Energy Transfer in the Presence of Lithium Ion, *J. Am. Chem. Soc.*, 2004, **126**(42), 13568–13569.
16 D. Citterio, J. Takeda, M. Kosugi, H. Hisamoto, S.-i. Sasaki, H. Komatsu and K. Suzuki, pH-Independent Fluorescent Chemosensor for Highly Selective Lithium Ion Sensing, *Anal. Chem.*, 2007, **79**(3), 1237–1242.
17 R. V. Hangarge, D. D. La, M. Boguslavsky, L. A. Jones, Y. S. Kim and S. V. Bhosale, An Aza-12-crown-4 Ether-Substituted Naphthalene Diimide Chemosensor for the Detection of Lithium Ion, *ChemistrySelect*, 2017, **2**(35), 11487–11491.
18 T. Gunnlaugsson, B. Bichell and C. Nolan, Fluorescent PET chemosensors for lithium, *Tetrahedron*, 2004, **60**(27), 5799–5806.
19 J.-H. Dong, C. Yang, H.-Q. Ding, P.-J. Xing, F.-Y. Zhou, H. Tian, X. Liu, H.-T. Zheng, S.-H. Hu and Z.-L. Zhu, Development of a Portable Method for Serum Lithium Measurement Based on Low-Cost Miniaturized Ultrasonic Nebulization Coupled with Atmospheric-Pressure Air-Sustained Discharge, *Anal. Chem.*, 2021, **93**(39), 13351–13359.
20 B. Valeur and I. Leray, Design principles of fluorescent molecular sensors for cation recognition, *Coord. Chem. Rev.*, 2000, **205**(1), 3–40.
21 E. Villemin and O. Raccurt, Optical lithium sensors, *Coord. Chem. Rev.*, 2021, **435**, 213801.
22 Z. R. Grabowski, K. Rotkiewicz and W. Rettig, Structural Changes Accompanying Intramolecular Electron Transfer: Focus on Twisted Intramolecular Charge-Transfer States and Structures, *Chem. Rev.*, 2003, **103**(10), 3899–4032.
23 A. P. De Silva, T. S. Moody and G. D. Wright, Fluorescent PET (Photoinduced Electron Transfer) sensors as potent analytical tools, *Analyst*, 2009, **134**(12), 2385–2393.
24 J. Fan, M. Hu, P. Zhan and X. Peng, Energy transfer cassettes based on organic fluorophores: construction and applications in ratiometric sensing, *Chem. Soc. Rev.*, 2013, **42**(1), 29–43.
25 A. C. Sedgwick, L. Wu, H.-H. Han, S. D. Bull, X.-P. He, T. D. James, J. L. Sessler, B. Z. Tang, H. Tian and J. Yoon, Excited-state intramolecular proton-transfer (ESIPT) based fluorescence sensors and imaging agents, *Chem. Soc. Rev.*, 2018, **47**(23), 8842–8880.
26 M. Kamenica, R. R. Kothur, A. Willows, B. A. Patel and P. J. Cragg, Lithium Ion Sensors, *Sensors*, 2017, **17**, 10.
27 R. A. Richards, K. Hammons, M. Joe and G. M. Miskelly, Observation of a Stable Water-Soluble Lithium Porphyrin, *Inorg. Chem.*, 1996, **35**(7), 1940–1944.
28 M. Tabata, J. Nishimoto and T. Kusano, Spectrophotometric determination of lithium ion using a water-soluble octabromoporphyrin in aqueous solution, *Talanta*, 1998, **46**(4), 703–709.
29 S. O. Obare and C. J. Murphy, A Two-Color Fluorescent Lithium Ion Sensor, *Inorg. Chem.*, 2001, **40**(23), 6080–6082.
30 M. McCarrick, S. J. Harris and D. Diamond, Assessment of three azophenol calix[4]arenes as chromogenic ligands for optical detection of alkali metal ions, *Analyst*, 1993, **118**(9), 1127–1130.
31 O. Santoro, M. R. J. Elsegood, S. J. Teat, T. Yamato and C. Redshaw, Lithium calix[4]arenes: structural studies and use in the ring opening polymerization of cyclic esters, *RSC Adv.*, 2021, **11**(19), 11304–11317.
32 C. J. Pedersen, Cyclic polyethers and their complexes with metal salts, *J. Am. Chem. Soc.*, 1967, **89**(10), 2495–2496.
33 B. P. Czech, D. A. Babb, B. Son and R. A. Bartsch, Functionalized 13-crown-4, 14-crown-4, 15-crown-4, and 16-crown-4 compounds: synthesis and lithium ion complexation, *J. Org. Chem.*, 1984, **49**(25), 4805–4810.
34 A. F. Danil de Namor, J. C. Y. Ng, M. A. Llosa Tanco and M. Salomon, Thermodynamics of Lithium–Crown Ether (12-crown-4 and 1-Benzyl-1-aza-12-crown-4) Interactions in Acetonitrile and Propylene Carbonate. The Anion Effect on the Coordination Process, *J. Phys. Chem.*, 1996, **100**(34), 14485–14491.
35 R. E. C. Torrejos, G. M. Nisola, H. S. Song, L. A. Limjuco, C. P. Lawagon, K. J. Parohinog, S. Koo, J. W. Han and W.-J. Chung, Design of lithium selective crown ethers: synthesis, extraction and theoretical binding studies, *Chem. Eng. J.*, 2017, **326**, 921–933.
36 A. Caballero, R. Tormos, A. Espinosa, M. D. Velasco, A. Tárraga, M. A. Miranda and P. Molina, Selective Fluorescence Sensing of Li^+ in an Aqueous Environment by a Ferrocene–Anthracene-Linked Dyad, *Org. Lett.*, 2004, **6**(24), 4599–4602.
37 S.-H. Kim, S.-K. Han, S.-H. Park, C.-M. Yoon and S.-R. Keum, Novel fluorescent chemosensor for Li^+ based on a squarylium dye carrying a monoazacrown moiety, *Dyes Pigm.*, 1999, **43**(1), 21–25.
38 M. Kollmannsberger, K. Rurack, U. Resch-Genger and J. Daub, Ultrafast Charge Transfer in Amino-Substituted Boron Dipyrromethene Dyes and Its Inhibition by Cation Complexation: A New Design Concept for Highly Sensitive Fluorescent Probes, *J. Phys. Chem. A*, 1998, **102**(50), 10211–10220.
39 Y. Ando, Y. Hiruta, D. Citterio and K. Suzuki, A highly Li^+-selective glass optode based on fluorescence ratiometry, *Analyst*, 2009, **134**(11), 2314–2319.

40 M.-S. Peng and J. Cai, Synthesis and fluorescence of crown ethers containing coumarin, *Dyes Pigm.*, 2008, **79**(3), 270–272.

41 M. Homocianu, A. M. Ipate, D. Homocianu, A. Airinei and C. Hamciuc, Metal ions sensing properties of some phenylquinoxaline derivatives, *Spectrochim. Acta, Part A*, 2019, **215**, 371–380.

42 F. Neese, Software update: The ORCA program system—Version 5.0, *Wiley Interdiscip. Rev.: Comput. Mol. Sci.*, 2022, e1606.

43 A. D. Becke, Density-functional thermochemistry. III. The role of exact exchange, *J. Chem. Phys.*, 1993, **98**(7), 5648–5652.

44 W. J. Hehre, R. Ditchfield and J. A. Pople, Self—Consistent Molecular Orbital Methods. XII. Further Extensions of Gaussian—Type Basis Sets for Use in Molecular Orbital Studies of Organic Molecules, *J. Chem. Phys.*, 1972, **56**(5), 2257–2261.

45 M. Al Kobaisi, S. V. Bhosale, K. Latham, A. M. Raynor and S. V. Bhosale, Functional Naphthalene Diimides: Synthesis, Properties, and Applications, *Chem. Rev.*, 2016, **116**(19), 11685–11796.

46 L. Ding, Z. Zhang, X. Li and J. Su, Highly sensitive determination of low-level water content in organic solvents using novel solvatochromic dyes based on thioxanthone, *Chem. Commun.*, 2013, **49**(66), 7319–7321.

47 P. Kumar, R. Kaushik, A. Ghosh and D. A. Jose, Detection of Moisture by Fluorescent Off-On Sensor in Organic Solvents and Raw Food Products, *Anal. Chem.*, 2016, **88**(23), 11314–11318.

48 H.-L. Qian, C. Dai, C.-X. Yang and X.-P. Yan, High-Crystallinity Covalent Organic Framework with Dual Fluorescence Emissions and Its Ratiometric Sensing Application, *ACS Appl. Mater. Interfaces*, 2017, **9**(29), 24999–25005.

49 K. Imato, T. Enoki and Y. Ooyama, Development of an intramolecular charge transfer-type colorimetric and fluorescence sensor for water by fusion with a juloidine structure and complexation with boron trifluoride, *RSC Adv.*, 2019, **9**(54), 31466–31473.

50 J. F. Hartwig, Evolution of a Fourth Generation Catalyst for the Amination and Thioetherification of Aryl Halides, *Acc. Chem. Res.*, 2008, **41**(11), 1534–1544.

51 P. Ruiz-Castillo and S. L. Buchwald, Applications of Palladium-Catalyzed C–N Cross-Coupling Reactions, *Chem. Rev.*, 2016, **116**(19), 12564–12649.

52 X.-X. Zhang and S. L. Buchwald, Efficient Synthesis of N-Aryl-Aza-Crown Ethers *via* Palladium-Catalyzed Amination, *J. Org. Chem.*, 2000, **65**(23), 8027–8031.

53 I. B. Berlman, 6—Graphs, in *Handbook of Fluorescence Spectra of Aromatic Molecules*, ed. I. B. Berlman, Academic Press, 2nd edn, 1971, pp. 107–415.

54 S. J. K. Pond, O. Tsutsumi, M. Rumi, O. Kwon, E. Zojer, J.-L. Brédas, S. R. Marder and J. W. Perry, Metal-Ion Sensing Fluorophores with Large Two-Photon Absorption Cross Sections: Aza-Crown Ether Substituted Donor−Acceptor−Donor Distyrylbenzenes, *J. Am. Chem. Soc.*, 2004, **126**(30), 9291–9306.

55 J. Li, Y. Lu, Q. Ye, M. Cinke, J. Han and M. Meyyappan, Carbon Nanotube Sensors for Gas and Organic Vapor Detection, *Nano Lett.*, 2003, **3**(7), 929–933.

56 I.-H. Chu, H. Zhang and D. V. Dearden, Macrocyclic chemistry in the gas phase: intrinsic cation affinities and complexation rates for alkali metal cation complexes of crown ethers and glymes, *J. Am. Chem. Soc.*, 1993, **115**(13), 5736–5744.

57 J. Warnock Samuel, R. Sujanani, S. Zofchak Everett, S. Zhao, J. Dilenschneider Theodore, G. Hanson Kalin, S. Mukherjee, V. Ganesan, D. Freeman Benny, M. Abu-Omar Mahdi and M. Bates Christopher, Engineering Li/Na selectivity in 12-Crown-4–functionalized polymer membranes, *Proc. Natl. Acad. Sci. U. S. A.*, 2021, **118**(37), e2022197118.